Global shifts in Noelaerhabdaceae assemblages during the late Oligocene-early Miocene

Julien Plancq[a*], Emanuela Mattioli[a], Jorijntje Henderiks[b], Vincent Grossi[a]

[a] Laboratoire de Géologie de Lyon (UMR 5276), CNRS, Université Lyon 1, Ecole Normale Supérieure Lyon, Campus scientifique de la DOUA, Villeurbanne, France

[b] Uppsala University, Department of Earth Sciences, Paleobiology Program, Villavägen 16, 752 36 Uppsala, Sweden

[*] Corresponding author : Julien Plancq, Laboratoire de Géologie de Lyon, UMR 5276, CNRS, Université Lyon 1, Campus de la DOUA, Bâtiment Géode, 69622 Villeurbanne Cedex, France. Tel.: +33 4 72431544.
E-mail address: julien.plancq@pepsmail.univ-lyon1.fr (J. Plancq)

This study investigates abundance variations in Noelaerhabdaceae assemblages during the late Oligocene-early Miocene at three subtropical sites in the Atlantic and Pacific oceans (DSDP Sites 516, 608 and 588). At these three sites, nannofossil assemblages were characterized by the successive high proportion of *Cyclicargolithus*, *Dictyococcites* and *Reticulofenestra*. Local paleoceanographic changes, such as the input of nutrient-poor water masses, might explain shifts in ecological prominence within the Noelaerhabdaceae at DSDP Site 516 (South Atlantic). But the similar timing of a decline in *Cyclicargolithus* at the three studied sites more likely corresponds to a global process. Here, we explore possible causes for this long-term taxonomic turnover. A global change in climate, associated with early Miocene glaciations, could have triggered a decline in fitness of the taxon *Cyclicargolithus*. The ecological niche made vacant because of the decrease in *Cyclicargolithus* could then have

been exploited by *Dictyococcites* and *Reticulofenestra* that became prominent in the assemblages after 20.5 Ma. Alternatively, this global turnover might reflect a gradual evolutionary succession and be the result of other selection pressures, such as increased competition between *Cyclicargolithus* and *Dictyococcites*/*Reticulofenestra*. A diversification within *Dictyococcites*/*Reticulofenestra*, indicated by an expansion in the size variation within this group since ~20.5 Ma, may have contributed to the decreased fitness of *Cyclicargolithus*.

Keywords: Noelaerhabdaceae; *Cyclicargolithus* decline; late Oligocene; early Miocene; climate; evolution.

1. Introduction

The Noelaerhabdaceae are a family of coccolithophores dominant in most Neogene calcareous nannofossil assemblages and includes the two most prominent modern coccolithophores and alkenone producers, namely *Emiliania huxleyi* and *Gephyrocapsa oceanica*, known to produce extensive blooms in today's oceans. Those large scale blooms have important implications for the global carbon cycle through processes of photosynthesis, calcification and respiration (Rost and Riebesell, 2004). During the Pleistocene, distinct intervals of dominance are recorded within the gephyrocapsids (e.g., Matsuoka and Okada, 1990; Bollmann et al., 1998; Flores and Marino, 2002; Flores et al., 2003; Baumann and Freitag, 2004; Barker et al., 2006) while *E. huxleyi* rose to global dominance ~270 thousand years ago (Thierstein et al., 1977). The cosmopolitan distribution of the Noelaerhabdaceae family, which is believed to represent the main lineage of ancient alkenone producers (Marlowe et al., 1990), was sustained throughout most of the Cenozoic. However, our

knowledge about the ecological preference or assemblage dynamics of the Oligocene and Miocene representatives of the Noelaerhabdaceae is relatively poor (Haq, 1980; Rio et al., 1990, Young, 1990; Kameo and Sato, 2000).

Several studies have shown that the late Oligocene-early Miocene period is marked by an important turnover of calcareous nannofossils, with first and last occurrences that are of biostratigraphic interest (Olafsson, 1989; Pujos, 1985; Young, 1998). For example, the early definition of the Oligocene-Miocene boundary relied on the last occurrence of *Dictyococcites bisectus* (*Reticulofenestra bisecta* of some authors; Berggren et al., 1985). However, only a few studies have estimated absolute abundances of the different genera of Noelaerhabdaceae during this period (e.g., Olafsson, 1989; Henderiks and Pagani, 2007; Plancq et al., 2012) and the paleoecological affinities of most species are still poorly known. The late Oligocene to early Miocene was a period of relative global warmth interrupted by large, transient Antarctic glaciations (named "Oi-2" and "Mi-1" events) as attested by significant oxygen isotopic ($\delta^{18}O$) increases (0.50 to >1.0 ‰) in benthic foraminiferal records (e.g., Miller et al., 1991, 1996; Zachos et al., 2001a,b; Billups et al., 2002). The opening and deepening of the Drake Passage and the subsequent intensification of the Antarctic Circumpolar Current (ACC) may have been coincident with the Oligocene-Miocene boundary and are believed to constitute important events in the Antarctic ice sheet expansion (e.g., Barker and Thomas, 2004; von der Heydt and Dijkstra, 2006), although the timing of this opening and causes of the inception of the glacial history of Antarctica are still being debated (Scher and Martin, 2006; Livermore et al., 2007; Cramer et al, 2009). The paleoceanographic changes associated with these cooling events could have influenced the composition of the nannofossil assemblages, which are largely controlled by variations in the temperature and nutrient characteristics of the upper water column (e.g., McIntyre and Bé, 1967; Okada and Honjo, 1973; Winter and Siesser, 1994).

In the present study, we investigate the relative and absolute abundances of three Noelaerhabdaceae genera - *Cyclicargolithus*, *Reticulofenestra* and *Dictyococcites* - in sediments from three Deep Sea Drilling Project (DSDP) sites covering the late Oligocene-early Miocene. These three sites are located in the North and South Atlantic and South-West Pacific, in areas corresponding to subtropical gyres. Results highlight similar variations in Noelaerhabdaceae assemblages at all studied sites, with an apparent global decline in *Cyclicargolithus*, a dominant species in Oligocene sediments, at ~20.5 million years ago (Ma). This overall turnover cannot be explained by local paleoceanographic changes alone, and suggests the influence of global abiotic and/or biotic selection pressures.

2. Material and methods

2.1. Studied sites and sampling strategy

The investigated time interval spans the latest Oligocene and the early Miocene, including nannofossil zones NP25-NN4 (Martini, 1971) (~25-16 Ma; Gradstein et al., 2012). Deep Sea Drilling Project (DSDP) Sites 516, 608 and 588 located in South Atlantic, North Atlantic and South-West Pacific respectively (Fig. 1), were selected for their continuous sedimentation and good nannofossil preservation (e.g., Barker et al., 1983; Lohman, 1986; Takayama and Sato, 1987; Plancq et al., 2012).

DSDP Leg 94 Site 608 (42°50N; 23°05W) is located on the eastern side of the North Atlantic Ridge on the southern flank of the King's Trough tectonic complex, at 3526 m water depth in the temperate subtropical North Atlantic gyre (Ruddiman et al., 1987). During the Miocene, Site 608 was at ca. 43°N (Wright et al., 1992) and nannofossil-foraminifera ooze deposition prevailed. Twenty-four samples were selected for this study, covering the nannofossil zones NN1-NN4 (Takayama and Sato, 1987).

DSDP Leg 90 Site 588 (26°06S; 161°E) was drilled on the Lord Howe Rise at 1533 m water depth in the South-West Pacific Ocean (Kennett et al., 1986). During the Miocene, this site was located at ca. 32.5°S (Wright et al., 1992), within a subtropical oligotrophic regime providing a steady nannofossil-foraminifera chalk sedimentation and upper water column stability (Flower and Kennett, 1993). Twenty-six samples were selected, across the nannofossil zones NP25-NN3 (Lohman, 1986).

DSDP Leg 72 Site 516 (30°16S; 35°17W) is located on the upper flanks of the Rio Grande Rise at 1313 m water depth in the South Atlantic subtropical gyre (Belkin and Gordon, 1996). This gyre has been located at the same latitude since the early Miocene (Barker et al., 1983). Sediments are primarily composed of nannofossil-foraminifera and nannofossil oozes. The thirty-six samples used for the present study are the same as those studied by Plancq et al. (2012), and cover nannofossil the zones NP25-NN4 (Barker et al., 1983).

Ages between each nannofossil zone refer to the latest geological timescale (Gradstein et al., 2012).

2.2. Micropaleontological analyses

Slides for calcareous nannofossil quantitative analysis were prepared following the random settling method (Beaufort, 1991; modified by Geisen et al., 1999). A small amount of dried sediment powder (5 mg) was mixed with water (with basic pH, over-saturated with respect to calcium carbonate) and the homogenized suspension was allowed to settle for 24 hours onto a cover slide. The slide was dried and mounted on a microscope slide with Rhodopass. Coccolith quantification was performed using a polarizing optical ZEISS microscope (magnification 1000x). A standard number of 500 calcareous nannofossils (coccoliths and nannoliths) were counted in a variable number of fields of views (between 10 and 30

123 according to the richness of the sample). Each slide was counted twice and the reproducibility
124 achieved was high (coefficient of variation: 10%).

125 Absolute abundance of nannofossils per gram of sediment was calculated using the
126 formula:

127 $$X = (N.V)/(M.A.H) \quad (1)$$

128 where X is the number of calcareous nannofossils per gram of sediment; N the number of
129 nannofossils counted in each sample; V the volume of water used for the dilution in the
130 settling device (cm^3); M the weight of powder used for the suspension (g); A the surface
131 considered for nannofossil counting (cm^2); H the height of the water over the cover slide in
132 the settling device (2.1 cm). Relative abundances (percentages) of nannofossil genera were
133 also calculated from the total nannofossil content.

134 The calculation of fluxes permits to overcome the effects of a variable sedimentary dilution
135 and to compare data from different intervals in a time-series. The formula introduced by
136 Davies et al. (1995) was used to calculate the mass accumulation rates (MAR):

137 $$MAR = T.\,[BD-(P.W)] \quad (2)$$

138 where MAR is the mass accumulation rate ($g/m^2/yr$), T the sedimentation rate (m/yr), BD the
139 wet bulk density (g/m^3), P the porosity (weight percent) and W the seawater density (1.025
140 g/cm^3).

141 Fluxes of nannofossils (specimens/m^2/yr) were then obtained by multiplying the MAR with
142 nannofossil abundances (specimens/g sediment).

143 Scanning electron microscope (SEM) images were taken using a field emission electron
144 microscope Zeiss Supra35VP, equipped with detectors for secondary and back-scattered
145 electrons.

146

147 **3. Taxonomy used for the Noelaerhabdaceae**

148

149 The taxonomy used to distinguish the different species within the Noelaerhabdaceae is
150 somewhat arbitrary, since it is primarily based on the coccolith size (Young, 1998). The
151 differentiation at the genus level of the three genera of the Noelaerhabdaceae
152 (*Reticulofenestra*, *Dictyococcites* and *Cyclicargolithus*) is also subject to discussion.
153 *Dictyococcites* is often considered as a junior synonym of *Reticulofenestra* and the two genera
154 are grouped either as reticulofenestrids (e.g., Henderiks and Pagani, 2007; Henderiks, 2008)
155 or more simply as *Reticulofenestra* (e.g., Young, 1998; Bolton et al., 2010). Nevertheless,
156 *Cyclicargolithus* represents a very characteristic genus easily distinguishable from other
157 reticulofenestrids due to its distinct shape (see Plate 1). In the present study, *Dictyococcites*,
158 *Reticulofenestra* and *Cyclicargolithus* were distinguished on the basis of distinctive
159 morphological features (see taxonomic remarks), and abundance variations are presented at
160 the genus level to establish the broad-scale patterns and facilitate a first-order comparison
161 between the investigated sites. Relative variations in size-defined morphospecies (see
162 taxonomic remarks), as well as previously published biometric datasets on *Reticulofenestra*,
163 *Dictyococcites* and *Cyclicargolithus* (Henderiks and Pagani, 2007; Plancq et al., 2012) at Site
164 516, further confirm our hypotheses of the long-term turnover within this prominent fossil
165 group.

166

167 **4. Results**

168

169 Mean absolute abundances of nannofossils at DSDP Sites 608, 516 and 588 are of the same
170 order of magnitude ($4.2x10^9$, $5.0x10^9$ and $5.4x10^9$ nannofossils/g of sediment, respectively),
171 and do not show any significant stratigraphic trend across the late Oligocene-early Miocene
172 (data not shown). Delicate coccoliths that are prone to dissolution, such as *Syracosphaera* and

Pontosphaera, although rare are observed with pristine structures in the samples investigated by light microscopy, indicating a good state of preservation of coccoliths at the three sites. Preservation of small coccoliths is also good, and coccospheres are commonly recorded (Plate 1). Observed coccolith assemblages are systematically dominated by four genera, which together account for more than 80% of the total nannofossil assemblage: *Reticulofenestra*, *Dictyococcites*, *Cyclicargolithus* (all belonging to the Noelaerhabdaceae), and *Coccolithus* (Figs. 2 and 3). These taxonomic groups are present throughout the investigated time interval. The same morphospecies occur at all three sites. In particular, *C. floridanus*, *R. pseudoumbilicus*, *R. minutula, R. haqii*, *R. minuta*, *D. antarcticus*, *D. hesslandii* and *Dictyococcites* smaller than 3 µm constitute on average more than 80% of the total nannofossil assemblage. Light microscopy and scanning electron microscopy (Plate 1) attest for a good preservation of Noelaerhabdaceae coccoliths.

Remarkably, for each genus of the Noelaerhabdaceae, relative abundances and fluxes show comparable temporal and quantitative variations at all sites (Figs. 2 and S1). *Cyclicargolithus* represents on average 27% of the total nannofossil assemblage before ~20.5 Ma (NP25-NN2) whereas it shows a sharp decrease in abundance (7% of the total nannofossil assemblage) after ~20.5 Ma (NN2-NN4). *Dictyococcites* shows significant quantitative variations throughout the studied time interval. Two peaks of maximum abundances are observed around 23 Ma (NN1) and between 20.5 and 18.5 Ma (36% of the total nannofossil assemblage; NN2-NN3). These variations are less obvious at Site 608, where no maximum is observed around 23 Ma, likely due to a lower resolution sampling during this period (Fig. 2). Finally, *Reticulofenestra* represents ca. 12% of the total nannofossil assemblage before ~20.5 Ma (NP25-NN2) but shows a progressive increase in abundance thereafter (29.5%), reaching more than 30% of the total nannofossil assemblage around 18 Ma (NN3).

Unlike Noelaerhabdaceae, abundances of *Coccolithus*, *Helicosphaera* and of the nannoliths *Sphenolithus* and *Discoaster* show distinct variations between the Atlantic and the Pacific oceans (Fig. 3). At both Atlantic sites, *Coccolithus* abundance is relatively constant (ca. 14.6% and 25% of the total nannofossil assemblage, for Sites 516 and 608, respectively) but shows a peak in abundance (36.5% for Site 516 and 46.6% for Site 608) between 20.5 and 18 Ma (NN2-NN3). The abundance of *Sphenolithus* is also relatively constant throughout the studied time interval (2% for Site 516; 8% for Site 608), and only shows a peak at ca. 18-17 Ma (NN3-NN4). This peak is less prominent at Site 516 (9.6%) than at Site 608 (21%). In the South-West Pacific (Site 588), *Coccolithus* is present in smaller proportions (10%) compared to both Atlantic sites (Fig. 3). Two small peaks of *Coccolithus* are observed within the nannofossil zone NN2 (17.8% and 20.7%) while the abundance of *Sphenolithus* shows no clear stratigraphic trend. The abundance of *Discoaster* is relatively constant throughout the studied time interval (5%), and only shows a peak (26%) at ca. 18 Ma at DSDP Site 608 (NN3). *Helicosphaera* shows low abundances (1.4%) and no peculiar stratigraphic trend (Fig. 3).

When considering relative abundances of different morphospecies within the Noelaerhabdaceae (Fig. 4), which together represent on average more than 80% of the total nannofossil assemblage, a distinct pattern of succession of prominent taxa is revealed. Namely, *Cyclicargolithus floridanus* (which is dominant with respect to *C. abisectus* showing average relative abundances < 2%) is very abundant in the three studied sites before ~20.5 Ma (NP25-NN2), with relative abundance fluctuations around 30%. It then fluctuates but shows generally values below 10%. *Reticulofenestra minuta* and *Dictyococcites* spp. (smaller than 3 µm) also show some of the highest values of relative abundance in the interval between 23 and 20.5 Ma (NN1-NN2), although a slightly different pattern is observed at the three sites. Between 20.5 and ~18 Ma (NN2-NN3), the morphospecies of intermediate size, namely *R.*

minutula and *D. hesslandii* did emerge as well as *D. antarcticus*. Finally, after 18 Ma (NN3-NN4), the larger morphospecies *R. pseudoumbilicus* (> 5 µm) shows abundance peaks up to 30% of the Noelaerhabdaceae.

The assemblage data for Site 516 are in agreement with those reported by Henderiks and Pagani (2007), although the apparent timing in assemblage shifts is slightly different due to different sample spacing in the two studies. The biometric data of Henderiks and Pagani (2007) and Plancq et al. (2012) for DSDP Site 516 show an increase in size in the reticulofenestrids that is in agreement with the morphospecies shifts we observe here at the three sites.

5. Discussion

Similar variations in Noelaerhabdaceae abundances are observed during the late Oligocene-early Miocene in the South and North Atlantic, and in the South-West Pacific (DSDP Sites 516, 608 and 588, respectively). At the three sites, nannofossil assemblages are successively characterized by high abundances of *Cyclicargolithus* before ~20.5 Ma, *Dictyococcites* between 20.5 and 18 Ma, and *Reticulofenestra* afterwards (Fig. 4). Within each genus, the number of morphospecies and their relative abundances varied over time and, to a lesser extent, between regions. Results are first discussed at genus level, then different-sized morphospecies changes are considered.

5.1. Changes in local paleoceanography and in calcareous nannofossil assemblages

The abundance changes within the Noelaerhabdaceae may represent distinct ecological responses of the different genera and species to local paleoceanographic changes. Although ecological preferences of Neogene nannofossils are poorly understood especially for the

246 Miocene, some hypotheses have been developed on the grounds of distribution patterns and
247 statistical analyses (e.g., Wei and Wise, 1990; Kameo and Sato, 2000; Monechi et al., 2000).
248 Henderiks and Pagani (2007) already discussed shifts in nannofossil assemblages at DSDP
249 Site 516 (Southern Atlantic) in response to paleoceanographic changes inferred from oxygen
250 isotopic ($\delta^{18}O$) values of foraminiferal tests and carbon isotopic ($\delta^{13}C$) compositions of
251 diunsaturated C_{37} alkenones (Pagani et al., 2000). The influx of warm, low-nutrient surface
252 waters from low latitudes may explain the decrease in *Cyclicargolithus* abundance between
253 ~21 and 20.5 Ma. This is consistent with the inferred ecological preference of this taxon,
254 which was apparently more abundant in mid paleo-latitudes (e.g., Wei and Wise, 1990) and
255 showed affinities for high-nutrient conditions (Monechi et al., 2000).
256 At ~20.3 Ma, an increased productivity of *Coccolithus*, and the subsequent prominence of
257 *Dictyococcites* (Figs. 2 and 3) may indicate the input of cold, nutrient-rich waters. An increase
258 in abundance of the genus *Dictyococcites* supports the presence of cold-water masses (Haq,
259 1980; Pujos, 1985; Kameo and Sato, 2000) during that time. *Coccolithus* is documented to
260 thrive at mid- and high-latitudes in both modern and ancient settings (Wei and Wise, 1990;
261 Wells and Okada, 1997; Cachão and Moita, 2000). This input of cold water has been
262 interpreted as a consequence of the opening of the Drake Passage to deeper-water, resulting in
263 an intensification of the Antarctic Circumpolar Current (ACC) and in a northward progression
264 of the Polar Frontal Zone (PFZ) (Barker and Burrell, 1977; Pagani et al., 2000). However, the
265 opening of the Drake Passage and a rapid deepening of the ACC may have occurred much
266 earlier in the late Eocene, at about 39-37 Ma (Scher and Martin, 2006; Livermore et al., 2007;
267 Cramer et al., 2009). In addition, Lagabrielle et al. (2009) have suggested a short-term closure
268 of the Drake Passage in the late Oligocene.
269 Following the cooling event, a re-establishment of surface water stratification (with
270 warmer waters) then induced the decline of *Dictyococcites* coupled to an increase of

Reticulofenestra and *Sphenolithus* (Figs. 2 and 3) after 19.5 Ma. *Reticulofenestra* spp. were more abundant at mid-to-high paleo-latitudes and were likely characteristic of mesotrophic, temperate water masses, while *Sphenolithus* appears to have been characteristic of warm/oligotrophic paleo-environments (e.g., Wei and Wise, 1990; Persico and Villa, 2004; Villa et al., 2008).

Noelaerhabdaceae assemblage shifts observed in the North Atlantic (DSDP Site 608) and the South-West Pacific (DSDP Site 588) are remarkably similar to those observed at Site 516, with a prominent decrease in *C. floridanus* proportions occurring at ~20 Ma and the parallel increase in some medium- and large-size reticulofenestrids (Fig. 4). However, DSDP Site 608 is located at mid-latitudes in the Northern Hemisphere, in a paleoceanographic setting far-removed from the ACC and from the PFZ, and paleoceanographic conditions at the Pacific Site 588 should have been particularly different from the two Atlantic sites during the studied time interval as suggested by the different trends observed in *Coccolithus* and *Sphenolithus* abundances (Fig. 3). Thus, the Noelaerhabdaceae variation pattern observed at the three sites cannot be explained by regional paleoceanographic changes alone.

5.2. Changes in climate and in calcareous nannofossil assemblages

The decline of *Cyclicargolithus* around 20.5 Ma (Figs. 2 and 4) may correspond to a more global feature. The successive dominance of *Cyclicargolithus*, *Dictyococcites* and *Reticulofenestra* may represent a passive ecological replacement in communities in response to a global shift in climate during the late Oligocene-early Miocene. The major decline of *Cyclicargolithus* would have allowed the expansion (and possibly diversification, see below) of *Dictyococcites*/*Reticulofenestra* into its vacant ecological niche, explaining the dominance of these species from 20.5 Ma onwards (Figs. 2 and 4).

In the Atlantic Ocean, Haq (1980) first observed a decrease in *Cyclicargolithus* assemblage between 22.5 and 18 Ma (within the NN2) and an increase in *Reticulofenestra*

296 *pseudoumbilicus-R. haqii* assemblage after 18 Ma. He suggested that this change in
297 nannofossil assemblages might result from changes in thermal structure of water masses and
298 steepening of latitudinal and vertical thermal gradients. Several Antarctic glaciations, called
299 "Oi-2" and "Mi-1" events, occurred during the late Oligocene to early Miocene period as
300 attested by excursions in $\delta^{18}O$ values of benthic foraminifers (e.g., Miller et al., 1991; Wright
301 and Miller, 1992). Interestingly, and despite the limited temporal resolution of the present
302 study, the onset of the decline of *Cyclicargolithus* may have coincided with Mi-1a and Mi-1aa
303 glacial events that occurred at about 21.3 and 20.2 Ma respectively (as shown by a ~0.5 ‰
304 increase in $\delta^{18}O$ values of benthic foraminifers; Wright and Miller, 1992; Paul et al., 2000;
305 Billups et al., 2002; Pekar and DeConto, 2006). The onset of such events could have changed
306 the oceanic circulation and surface water characteristics influencing the ecology and thus
307 composition of the nannofossil assemblages. For example, at DSDP Site 516, Pagani et al.
308 (2000) hypothesized that the Mi-1a event led to an intensification of gyre circulation in South
309 Atlantic and thus to a higher influx of warm, low-nutrient waters from lower latitudes, which
310 may have triggered the decline of *Cyclicargolithus* observed at this site. The Mi-1a event is
311 recorded in $\delta^{18}O$ data at DSDP Sites 608 and 588 (Kennett, 1985; Woodruff and Savin, 1989;
312 Wright et al., 1992; Norris et al., 1994), but evidence is lacking for a global change in oceanic
313 circulation that could have affected the paleoceanography of the North Atlantic and South-
314 West Pacific in similar ways. Specific orbital configuration (high-amplitude variability in
315 obliquity) coupled to variability in atmospheric carbon dioxide may explain the onset of Mi-1
316 events (e.g. Zachos et al., 2001b; Pälike et al., 2006). For example, the Mi-1a event may have
317 accounted for a ~50 ppmv decrease in partial pressure of atmospheric carbon dioxide (pCO_2)
318 as recorded in the ^{13}C content of alkenones at DSDP Sites 516, 588 and 608 (Pagani et al.,
319 1999, 2000) and, at a more global scale, by stomatal frequency data (stomatal index) from
320 multiple tree species (Kürschner et al., 2008). Atmospheric CO_2 is believed to have a strong

influence on the long-term climate evolution. Nevertheless, considering the error propagation of the available proxies, atmospheric CO_2 concentrations are actually surprisingly stable during the Miocene and it seems difficult to relate a global shift in climate with an apparent small fluctuation in pCO_2 (Pagani et al., 1999, 2000). This issue remains puzzling and debated in light of the climatic and ecological events that occurred during the Miocene (e.g., Pagani, 2002; Pagani et al., 2009; LaRiviere et al., 2012).

Supplementary evidence is thus needed to support the hypothesis that the global turnover in Noelaerhabdaceae assemblages is linked to a global climatic change (variations in oceanic circulation and/or influence of atmospheric pCO_2).

5.3. Changes within the Noelaerhabdaceae

Alternatively, the successive dominance of *Cyclicargolithus*, *Dictyococcites* and *Reticulofenestra* could be the result of other selection pressures within the phytoplankton communities. The Oligocene-Miocene transition is characterized by an important turnover in nannofossils assemblages, notably within the Noelaerhabdaceae with the last occurrence of *Reticulofenestra bisecta* (Okada and Bukry, 1980; Berggren et al., 1985; Young, 1998). Climatic perturbations could have sped up the race for being the fittest species and the steady increase in abundance of *Dictyococcites*/*Reticulofenestra* might be the effect of an active competition between the two groups (*Cyclicargolithus*, mainly *C. floridanus*, and *Dictyococcites*/*Reticulofenestra*), rather than a passive exploitation by these species of the ecological niche made vacant because of the decrease of *Cyclicargolithus*. Biometry data suggest a distinct diversification in *Dictyococcites*/*Reticulofenestra* after 20.5 Ma at Site 516 (Henderiks and Pagani, 2007; Plancq et al., 2012). The present results show that, in the three studied sites after 20.5 Ma, there is an increase in the relative abundance of morphospecies of intermediate and large size that mirrors the decline in *C. floridanus* (Fig. 4). This increase in abundance of large morphospecies of *Dictyococcites*/*Reticulofenestra* that became more

prominent with time may correspond to cryptic speciation within the group: minor size differences can characterize cryptic species in modern coccolithophores (for a synthesis, see Geisen et al., 2004). Interestingly, similar successions in species dominance have been observed for younger members of the Noelaerhabdaceae family, in particular within the *Gephyrocapsa* complex during the Quaternary, whose biometric changes have been interpreted in terms of evolutionary adaptation for lack of a clear linkage to concurrent changes in climate and/or preservation (e.g., Matsuoka and Okada, 1989; 1990; Bollmann et al., 1998). A diversification in *Dictyococcites*/*Reticulofenestra* may have induced the steady decline (occurring over ~1 Ma; Fig. 4) of *Cyclicargolithus floridanus*, although this taxon maintained competitive populations until its extinction occurring 8 Myr later (last occurrence at 11.85 Ma; Gradstein et al., 2012).

6. Conclusion

Similar relative and absolute abundance variations in Noelaerhabdaceae assemblages are observed during the late Oligocene-early Miocene in subtropical regions of the Atlantic and Pacific oceans, with the successive prominence of *Cyclicargolithus floridanus*, *Dictyococcites antarcticus*/*D. hesslandii*, and *Reticulofenestra minutula* /*R. pseudoumbilicus*. We explored the paleoenvironmental factors that may have triggered the observed assemblage turnover, in spite of a poor knowledge of the ecological preferences of the Oligocene-Miocene species/genera and of the rather arbitrary, size-defined taxonomy of the Noelaerhabdaceae family. The decline of *Cyclicargolithus* recorded at the three studied sites may correspond to a global climatic shift (variations in oceanic circulation or influence and/or atmospheric pCO_2) eventually coupled to variations in local paleoceanographic conditions. The subsequent dominance of *Dictyococcites and Reticulofenestra* in assemblages after ~20.5 Ma is paired

371 with a diversification in coccolith sizes, and may be the result of an evolutionary process such
372 as competition between the two groups (*Cyclicargolithus* and
373 *Dictyococcites*/*Reticulofenestra*). The present study confirms that changes in nannofossil
374 assemblages are a good proxy for the reconstruction of global evolutionary patterns that may
375 be related to paleoenvironmental changes. However, morphospecies biometry and
376 paleoceanographic studies at higher temporal resolution, depicting both paleoecological and
377 evolutionary patterns, will be needed to reinforce the presented hypotheses for the global
378 shifts in Noelaerhabdaceae assemblages.

379

380 **Acknowledgements**

381

382 We would like to thank Jeremy Young, Giuliana Villa and Richard Jordan for their
383 constructive comments and critical review of a previous version of the manuscript. This study
384 used Deep Sea Drilling Project samples provided by the Integrated Ocean Drilling Program.
385 We thank the curators from the Bremen Core Repository and the Kochi Core Center for their
386 efficiency. Yannick Donnadieu (LSCE, France) is kindly acknowledged for stimulating
387 discussions.

388

389 **References**

390

391 Backman, J., 1980. Miocene-Pliocene nannofossils and sedimentation rates in the Hatton-
392 Rockall Basin, NE Atlantic Ocean. Stockholm Contributions in Geology 36, 1-91.
393 Barker, P.F., Burrell, J., 1977. The opening of the Drake Passage. Marine Geology 25, 15–34.

394 Barker P.F., Carlson, R.L., Johnson, D.A., the Shipboard Scientific Party, 1983. Site 516: Rio
395 Grande Rise. Initial Reports of Deep Sea Drilling Project 72, 155-338,
396 doi:10.2973/dsdp.proc.72.105.
397 Barker, P.F., Thomas, E., 2004. Origin, signature and palaeoclimatic influence of the
398 Antarctic circumpolar current. Earth Science Reviews 66, 143-162.
399 Barker, S., Archer, D., Booth, L., Elderfield, H., Henderiks, J., Rickaby, R.E.M., 2006.
400 Globally increased pelagic carbonate production during the Mid-Brunhes dissolution
401 interval and the CO_2 paradox of MIS 11. Quaternary Science Reviews 25, 3278-3293.
402 Baumann, K-H., Freitag, T., 2004. Pleistocene fluctuations in the northern Benguela Current
403 system as revealed by coccolith assemblages. Marine Micropaleontology 52, 195-215.
404 Beaufort, L., 1991. Adaptation of the random settling method for quantitative studies of
405 calcareous nannofossils. Micropaleontology 37, 415–418.
406 Belkin, I.M., Gordon, A.L., 1996. Southern Ocean fronts from the Greenwich meridian to
407 Tasmania. Journal of Geophysical Research 101, 3675– 3696.
408 Berggren, W.A., Kent, D.V., Flynn, J., Van Couvering, J.A., 1985. Cenozoic geochronology.
409 Geological Society of America Bulletin 96, 1407–1418.
410 Billups, K., Channell, J.E.T., Zachos, J., 2002. Late Oligocene to early Miocene
411 geochronology and paleoceanography from the subantarctic South Atlantic.
412 Paleoceanography 17 (1), 1004, doi:10.1029/2000PA000568.
413 Bollmann, J., Baumann , K.H., Thierstein, H.R., 1998. Global dominance of *Gephyrocapsa*
414 coccoliths in the late Pleistocene: selective dissolution, evolution, or global environmental
415 change? Paleoceanography 13, 517-529.
416 Bolton, C.T., Lawrence, K.T., Gibbs, S.J., Wilson, P.A., Cleaveland, L.C., Timothy, D.,
417 Herbert, T.D., 2010. Glacial-interglacial productivity changes recorded by alkenones and

418 microfossils in late Pliocene eastern equatorial Pacific and Atlantic upwelling zones. Earth
419 and Planetary Science Letters 295, 401-411.
420 Bukry, D., 1971. Cenozoic calcareous nannofossils from the Pacific Ocean. Transactions of
421 the San Diego Society of Natural History 16, 303-327.
422 Cachão, M., Moita, M.T., 2000. *Coccolithus pelagicus*, a productivity proxy related to
423 moderate fronts off Western Iberia. Marine Micropaleontology 39, 131– 155.
424 Cramer, B.S., Toggweiler, J.R., Wright, J.D., Katz, M.E., Miller, K.G., 2009. Ocean
425 overturning since the Late Cretaceous : inferences from a new benthic foraminiferal
426 isotope compilation. Paleoceanography 24, doi: 10.1029/2008PA001683.
427 Davies, T.A., Kidd, R.B., Ramsay-Anthony, T.S., 1995. A time-slice approach to the history
428 of Cenozoic sedimentation in the Indian Ocean. In: T.A. Davies, M.F. Coffin, and S.W.
429 Wise (Eds.), Selected Topics Relating to the Indian Ocean Basins and Margins,
430 Sedimentary Geology 96, 157–179.
431 Flores, J.A., Marino, M., 2002. Pleistocene calcareous nannofossil stratigraphy for ODP Leg
432 177 (Atlantic sector of the Southern Ocean). Marine Micropaleontology 45, 191–224.
433 Flores, J.A., Marino, M., Sierro, F.J., Hodell, D.A., Charles, C.D., 2003. Calcareous plankton
434 dissolution pattern and coccolithophore assemblages during the last 600 kyr at ODP Site
435 1089 (Cape Basin, South Atlantic): paleoceanographic implications. Paleogeography,
436 Paleoclimatology, Paleoecology 196, 409-426.
437 Flower, B.P., Kennett, J.P., 1993. Middle Miocene ocean–climate transition: high resolution
438 oxygen and carbon isotopic records from DSDP Site 588A, southwest Pacific.
439 Paleoceanography 8, 811–843.
440 Geisen, M., Bollmann, J., Herrle, J.O., Mutterlose, J., Young, J.R., 1999. Calibration of the
441 random settling technique for calculation of absolute abundance of calcareous
442 nannoplankton. Micropaleontology 45 (4), 437-442.

Geisen, M., Young, J.R., Probert, I., Saez, A.G., Baumann, K.-H., Bollmann, J., Cros, L., de Vargas, C., Medlin, L.K., Sprengel, C., 2004. Species level variations in coccolithophores. In: H.R. Thierstein, and J.R. Young (Eds.), Coccolithophores, from molecular processes to global impact, Springer, 327-367 pp.

Gradstein, F.M., Ogg, J.G., Schmitz, M., Ogg, G., 2012. The Geologic Time Scale 2012. Elsevier, 1176 pp.

Haq, B.U., 1976. Coccoliths in cores from the Bellinghausen abyssal plain and Antarctic continental rise (DSDP Leg 35). Initial Reports of Deep Sea Drilling Project 35, 557-567.

Haq, B.U., 1980. Biogeographic history of Miocene calcareous nannoplankton and paleoceanography of the Atlantic Ocean. Micropaleontology 26 (4), 414-443.

Henderiks, J., 2008. Coccolithophore size rules-reconstructing ancient cell geometry and cellular calcite quota from fossil coccoliths. Marine Micropaleontology 67, 143-154.

Henderiks, J., Pagani, M., 2007. Refining ancient carbon dioxide estimates: significance of coccolithophore cell size for alkenone-based pCO_2 records. Paleoceanography 22, PA3202, doi: 10.1029/2006PA001399.

Jordan, R.W., Cros, L., Young, J.R., 2004. A revised classification scheme for living haptophytes. Micropaleontology 50, 55-79.

Kameo, K., Sato, T., 2000. Biogeography of Neogene calcareous nannofossils in the Caribbean and the eastern equatorial Pacific-floral response to the emergence of the Isthmus of Panama. Marine Micropaleontology 39, 201-218.

Kennett, J.P., 1985. Miocene to early Pliocene oxygen and carbon isotope stratigraphy in the southwest Pacific, Deep Sea Drilling Project Leg 90. Initial Reports of Deep Sea Drilling Project 90, 1383-1411, doi:10.2973/dsdp.proc.90.142.

Kennett, J.P., von der Borch, C.C., the Shipboard Scientific Party, 1986. Site 588: Lord Howe Rise, 26°S. Initial Reports of Deep Sea Drilling Project 90, 139-252, doi:10.2973/dsdp.proc.90.104.

Kürschner, W.M., Kvaček, Z., Dilcher, D.L., 2008. The impact of Miocene atmospheric carbon dioxide fluctuations on climate and the evolution of terrestrial ecosystems. Proceedings of the National Academy of Science U.S.A. 105 (2), 449-453.

Lagabrielle, Y., Goddéris, Y., Donnadieu, Y., Malavieille, J., Suarez, M., 2009. The tectonic history of Drake Passage and its possible impacts on global climate. Earth and Planetary Science Letters 279, 197-211.

LaRiviere, J.P., Ravelo, A.C., Crimmins, A., Dekens, P.S., Ford, H.L., Lyle, M., Wara, M.W., 2012. Late Miocene decoupling of oceanic warmth and atmospheric carbon dioxide forcing. Nature 486, 97-100.

Livermore, R., Hillenbrand, C-D., Meredith, M., Eagles G., 2007. Drake Passage and Cenozoic climate: an open shut case? Geochemistry, Geophysics, Geosystems 8(1), doi: 10.1029/2005GC001224.

Lohman, W.H., 1986. Calcareous nannoplankton biostratigraphy of the southern Coral sea, Tasman Sea, and southwestern Pacific Ocean, Deep Sea Drilling Project Leg 90: Neogene and Quaternary. Initial Reports of Deep Sea Drilling Project 90, 763-793, doi:10.2973/dsdp.proc.90.112.

Marlowe, I.T., Brassell, S.C., Eglinton, G., Green, J.C., 1990. Long-chain alkenones and alkyl alkenoates and the fossil coccolith record of marine sediments. Chemical Geology 88, 349-375.

Martini, E., 1971. Standard Tertiary and Quaternary calcareous nannoplankton zonation. In: Farinacci, A. (Ed.), Proceedings of the second planktonic conference 2, 739-785 pp.

Matsuoka, H., Okada, H., 1989. Quantitative analysis of Quaternary nannoplankton in the subtropical northwestern Pacific Ocean. Marine Micropaleontology 14, 97-118.

Matsuoka, H., Okada, H., 1990. Time-progressive morphometrical changes of the genus *Gephyrocapsa* in the Quaternary sequence of the tropical Indian Ocean, Site 709. In: Duncan, R.A., Backman, J., Peterson, L.C. et al. (Eds.), Proceedings of the Ocean Drilling Program Scientific Results 115, 255-270.

McIntyre, A., Bé, A.W.H., 1967. Modern coccolithophores of the Atlantic Ocean-I. Placolith and cyrtoliths. Deep-Sea Research 14, 561-597.

Miller, K.G., Wright, J.D., Fairbanks, R.G., 1991. Unlocking the ice house: Oligocene to Miocene oxygen isotopes, eustasy, and margin erosion. Journal of Geophysical Research 96, 6829-6848.

Miller, K.G., Mountain, G.S., and Leg 150 Shipboard Party and Members of the New Jersey Coastal Plan Drilling Project, 1996. Drilling and dating New Jersey Oligocene-Miocene sequences: ice volume, global sea level, and EXXON records. Science 271, 1092-1095.

Monechi, S., Buccianti, A., Gardin, S., 2000. Biotic signals from nannoflora across the iridium anomaly in the upper Eocene of the Massignano section: evidence from statistical analysis. Marine Micropaleontology 39, 219-237.

Norris, R.D., Corfield, R.M., Cartlidge, J.E., 1994. Evolutionary ecology of *Globorotalia* (*Globoconella*) (planktic foraminifera). Marine Micropaleontology 23, 121-145.

Okada, H., Bukry, D., 1980. Supplementary modification and introduction of code numbers to the low-latitude coccolith biostratigraphic zonation (Bukry, 1973; 1975). Marine Micropaleontology 5, 321-325.

Okada, H., Honjo, S., 1973. The distribution of oceanic coccolithophorids in the Pacific. Deep-Sea Research 20, 335–374.

514 Olafsson, G., 1989. Quantitative calcareous nannofossil biostratigraphy of upper Oligocene to
515 middle Miocene sediment from ODP Hole 667A and middle Miocene sediment from
516 DSDP site 574. Proceedings of the Ocean Drilling Program Scientific Results 108, 9-22.
517 Pagani, M., 2002. The alkenone-CO_2 proxy and ancient atmospheric carbon dioxide.
518 Philosophical Transactions of the Royal Society A 360, 609-632.
519 Pagani, M., Arthur, M.A., Freeman, K.H., 1999. Miocene evolution of atmospheric carbon
520 dioxide. Paleoceanography 14 (3), 273-292.
521 Pagani, M., Arthur, M.A., Freeman, K.H., 2000. Variations in Miocene phytoplankton growth
522 rates in the southwest Atlantic: evidence for changes in ocean circulation.
523 Paleoceanography 15, 486-496.
524 Pagani, M., Caldeira, K., Berner, R., Beerling, D.J., 2009. The role of terrestrial plants in
525 limiting atmospheric CO_2 decline over the past 24 million years. Nature 460, 85-89.
526 Pälike, H., Frazier, J., Zachos, J.C., 2006. Orbitally forced palaeoclimatic records from the
527 equatorial Atlantic Ceara Rise. Quaternary Science Reviews 25, 3138-3149.
528 Paul, H.A., Zachos, J.C., Flower, B.P., Tripati, A., 2000. Orbitally induced climate and
529 geochemical variability across the Oligocene/Miocene boundary. Paleoceanography 15,
530 471-485.
531 Pekar, S.F., DeConto, R.M., 2006. High-resolution ice-volume estimates for the early
532 Miocene: evidence for a dynamic ice sheet in Antarctica. Palaeogeography,
533 Palaeoclimatology, Palaeoecology 231, 101-109.
534 Persico, D., Villa, G., 2004. Eocene–Oligocene calcareous nannofossils from Maud Rise and
535 Kerguelen Plateau (Antarctica): paleoecological and paleoceanographic implications.
536 Marine Micropaleontology 52, 153-179.

Plancq, J., Grossi, V., Henderiks, J., Simon, L., Mattioli, E., 2012. Alkenone producers during late Oligocene-early Miocene revisited. Paleoceanography 27, PA1202, doi: 10.1029/2011PA002164.

Pujos, A., 1985. Late Eocene to Pleistocene medium-sized and small-sized Reticulofenestrids. In: H. Stradner, and K. Perch-Nielsen (Eds.), Proc. INA meeting, Vienna 1985, Abhandlungen der Geologischen Bundesanstalt 39, 239–277.

Rost, B., Riebesell, U., 2004. Coccolithophores and the biological pump: responses to environmental changes. In: H.R. Thierstein, and J.R. Young (Eds), Coccolithophores – From Molecular Processes to Global Impact, Springer, New York, 76-99.

Ruddiman, W.F., Kidd, R.B., Thomas, E., the Shipboard Scientific Party, 1987. Site 608. Initial Reports of Deep Sea Drilling Project 94, 149-246, doi:10.2973/dsdp.proc.94.104.

Scher, H.D., Martin, E.E., 2006. Timing and climatic consequences of the opening of Drake Passage. Science 312, 428-430.

Takayama, T., Sato, T., 1987. Coccolith biostratigraphy of the North Atlantic Ocean, Deep Sea Drilling Project Leg 94. Initial Reports of Deep Sea Drilling Project 94, 651-702, doi:10.2973/dsdp.proc.94.113.

Theodoridis, S.A., 1984. Calcareous nannofossil biozonation of the Miocene and revision of the helicoliths and discoasters. Utrecht Micropaleontological Bulletins 32, 32-271.

Thierstein, H.R., Geitzenauer, K.R., Molfino, B., Shackleton, N.J., 1977. Global synchroneity of late Quaternary coccolith datum levels: Validation by oxygen isotopes. Geology 5, 400-404.

Villa, G., Fioroni, C., Pea, L., Bohaty, S., Persico, D., 2008. Middle Eocene–late Oligocene climate variability: Calcareous nannofossil response at Kerguelen Plateau, Site 748. Marine Micropaleontology 69, 173-192.

561 von der Heydt, A., Dijkstra, H.A., 2006. Effect of ocean gateways on the global ocean
562 circulation in the late Oligocene and early Miocene. Paleoceanography 21, PA10111,
563 doi:10.1029/2005PA001149.
564 Wei, W., Wise, S.W., 1990. Biogeographic gradients of middle Eocene-Oligocene calcareous
565 nannoplankton in the South Atlantic Ocean. Palaeogeography, Palaeoclimatology,
566 Palaeoecology 79, 29-61.
567 Wells, P., Okada, H., 1997. Response of nannoplankton to major changes in sea-surface
568 temperature and movements of hydrological fronts over Site DSDP 594 (south Chatham
569 Rise, southeastern New Zeland), during the last 130 Kyr. Marine Micropaleontology. 32,
570 341–363.
571 Winter, A., Siesser, W., 1994. Coccolithophores. Cambridge University Press, Cambridge,
572 242 pp.
573 Woodruff, F., Savin, S.M., 1989. Miocene deep water oceanography. Paleoceanography 4,
574 87-140.
575 Wright, J.D., Miller, K.G., 1992. Miocene stable isotope stratigraphy, site 747, Kerguelen
576 Plateau. Proceedings of the Ocean Drilling Program Scientific Results 120, 855-866.
577 Wright, J.D., Miller, K.G., Fairbanks, R.G., 1992. Early and middle Miocene stable isotopes:
578 implications for deepwater circulation and climate. Paleoceanography 7, 357-389.
579 Young, J.R., 1990. Size variation of Neogene *Reticulofenestra* coccoliths from Indian Ocean
580 DSDP cores. Journal of Micropaleontology 9, 71-86.
581 Young, J.R., 1998. Neogene. In: P.R. Bown (Ed.), Calcareous Nannofossil Biostratigraphy.
582 Chapman and Hall, Cambridge, U.K, pp. 225-265.
583 Young, J.R., Bown, P.R., 1997. Cenozoic calcareous nannoplankton classification. Journal of
584 Nannoplankton Research 19, 36-47.

Young, J.R., Geisen, M., Cros, L., Kleijne, A., Probert, I., Sprengel, C., Ostergaard, J.B., 2003. A guide to extant coccolithophore taxonomy. Journal of Nannoplankton Research Special Issue 1, 1–132.

Zachos, J.C., Pagani, M., Sloan, L., Thomas, E., Billups, K., 2001a. Trends, rhythms, and aberrations in global climate 65 Ma to present. Science 292, 686-693.

Zachos, J.C., Shackleton, N.J., Revenaugh, J.S., Pälike, H., Flower, B.P., 2001b. Climate response to orbital forcing across the Oligocene-Miocene boundary. Science 292, 274-278.

Appendix A. Taxonomic remarks

Taxonomy used in the present work follows haptophyte phylogeny as revised by Young and Bown (1997), Young et al. (2003) and Jordan et al. (2004).

A1. Family Noelaerhabdaceae Jerkovic 1970 emend. Young & Bown 1997

This is the dominant family in most Neogene assemblages, and includes the extant genera *Emiliania* and *Gephyrocapsa*.

A1.1. Genus Reticulofenestra Hay, Mohler and Wade 1966

Elliptical to sub-circular reticulofenestrids with a prominent open central area, and with no slits in the distal shield. The rather simple morphology of *Reticulofenestra* makes subdivision into species notoriously problematic. The conventional taxonomy is primarily based on size. This is unsatisfactory and arbitrary, but of stratigraphic value (Backman, 1980; Young, 1990). In this study, a subdivision of four species based on size and central area opening size was employed during the assemblage counts:

Reticulofenestra haqii Backman 1978: morphospecies 3-5 µm in length, with a central opening shorter than 1.5 µm.

610 *Reticulofenestra minuta* Roth 1970: morphospecies smaller than 3 µm.

611 *Reticulofenestra minutula* (Gartner 1967) Haq and Berggren 1978: morphospecies 3-5 µm in
612 length with a central opening longer than 1.5 µm.

613 *Reticulofenestra pseudoumbilicus* (Gartner 1967) Gartner 1969: larger morphospecies (> 5~~–7~~
614 µm).

615

616 *A1.2. Genus Dictyococcites (Black 1967) emend. Backman 1980*

617 Elliptical reticulofenestrids with a large central area closed (or virtually closed) in line with
618 the distal shield. The central area of the distal shield frequently shows a median furrow or a
619 minute pore, but not large enough to suggest that they belong to *Reticulofenestra*. Although
620 *Dictyococcites sensu* Black (1967) can be regarded as a heavily calcified, junior synonym of
621 *Reticulofenestra*, the emended diagnosis of Backman (1980) allows consistent separation of
622 this genus from *Reticulofenestra*.

623 *Dictyococcites* sp.: small morphospecies (< 3 µm) with a closed central area.

624 *Dictyococcites antarcticus* Haq 1976: in contrast with *D. hesslandii*, the specimens of *D.*
625 *antarcticus* (4-8 µm) show no pore but a narrow and elongated rectangular central area
626 (named "furrow" in Haq, 1976 and "straight band" in Backman, 1980). The straight extinction
627 band along the major axis occupies at least one half of the total length of the elliptical central
628 area (Backman, 1980).

629 *Dictyococcites hesslandii* (Haq 1966) Haq and Lohmann 1976: the central area of the distal
630 shield exhibits a small pore, from which extinction bands radiate (3-8 µm).

631

632 *A1.3. Genus Cyclicargolithus Bukry 1971*

633 Circular to sub-circular reticulofenestrids with a small central area and high tube-cycles.
634 Although Theodoridis (1984) regarded *Cyclicargolithus* as a junior synonym of

635 *Reticulofenestra*, the diagnosis of Bukry (1971) allows consistent separation of this genus
636 from *Reticulofenestra*.
637 *Cyclicargolithus abisectus* (Müller 1970) Wise 1973: large species (>10 µm).
638 *Cyclicargolithus floridanus* (Roth and Hay in Hay et al., 1967) Bukry 1971: species smaller
639 than 10 µm.
640
641 **A2. Other coccoliths recorded in this study**
642 *Calcidiscus leptoporus* (Murray and Blackman 1898) Loeblich and Tappan 1978
643 *Coccolithus miopelagicus* Bukry 1971
644 *Coccolithus pelagicus* (Wallich 1877) Schiller 1930
645 *Helicosphaera* spp. Kamptner 1954
646 *Pontosphaera* spp. Lohmann 1902
647 *Syracosphaera pulchra* Lohmann 1902
648 *Umbilicosphaera* spp. Lohmann 1902
649
650 **A3. Nannoliths**
651 *Discoaster* spp. Tan 1927
652 *Sphenolithus* spp. Deflandre in Grassé 1952
653
654 **Figure captions**
655
656 **Figure 1.** Location of the studied DSDP Sites 608, 516 and 588.
657
658 **Figure 2.** Relative abundances (%) of the Noelaerhabdaceae genera (*Cyclicargolithus*,
659 *Dictyococcites* and *Reticulofenestra*) during the late Oligocene-early Miocene at the three

studied sites. Data is plotted against depth in core (mbsf: meters below sea floor) and the nannofossil zonation of Martini (1971), calibrated to the timescale of Gradstein et al. (2012). Note that positions (in dashed lines) of the zonal boundaries between NN2-NN3 and NN1-NN2 are uncertain at Site 608 and Site 588, respectively. For the three studied sites, the decline of *Cyclicargolithus* occurred at about 20.5 Ma (position estimated based on the nannofossil zonation). LO: Late Oligocene.

Figure 3. Relative abundances (%) of *Coccolithus*, *Helicosphaera* and of the nannoliths *Sphenolithus* and *Discoaster* at DSDP Sites 516, 608 and 588 during the late Oligocene-early Miocene. LO: Late Oligocene; Mbsf: meters below sea floor. Nannofossil zonation as described in Fig. 2.

Figure 4. Relative abundances (%) of the different species within the Noelaerhabdaceae at DSDP Sites 516, 608 and 588 during the late Oligocene-early Miocene. Gray colors indicate different time intervals in which, although small differences are observed between the three sites, similar changes in the relative abundance of species occurred. The first interval, before ~20.5 Ma (NP25-NN2), is characterized by the dominance of *Cyclicargolithus floridanus*. The second interval (between ~20.5 and ~18 Ma; NN2-NN3) is marked by higher abundance of *D. antarcticus*, *D. hesslandii* and *R. minutula*. The third interval, after 18 Ma (NN3-NN4), is defined by the emergence of *R. pseudoumbilicus*.

Plate 1. Images in cross-polarized light (POL) and scanning electron microscope (SEM) of the three genera of the Noelaerhabdaceae during the late Oligocene-early Miocene. **a)** *Reticulofenestra minutula*, POL (1000x), Sample 608-39H3-127 and 588C-5R2-25. **b-c)** *Reticulofenestra minuta*, SEM, Sample 588C-2R6-100. **d)** *Reticulofenestra pseudoumbilicus*,

SEM, Sample 516F-10R1-122. **e)** *Dictyococcites* sp., POL (1000x), Sample 516-27H3-79. **f)** *Dictyococcites antarcticus*, POL (1000x), Sample 588C-4R5-33. **g)** *Dictyococcites hesslandii*, SEM, Sample 588C-11R1-111. **h)** *Dictyococcites antarcticus*, SEM, 516F-10R1-122. **i)** *Dictyococcites* sp., SEM, Sample 588C-11R1-111. **j)** *Dictyococcites hesslandii* (coccosphere), SEM, Sample 516-26H2-18. **k-l)** *Cyclicargolithus floridanus*, POL (1000x), Sample 516-26H2-18 and 588C-2R6-100. **m-n)** *Cyclicargolithus floridanus*, SEM, Sample 588C-2R6-100 and 516F-10R1-53. Scale bars: 1µm.

Supplementary data

Figure S1. Fluxes (coccoliths/m^2/yr) of the Noelaerhabdaceae genera (*Cyclicargolithus*, *Dictyococcites* and *Reticulofenestra*) during the late Oligocene-early Miocene at the three studied sites. Data is plotted against depth in core (mbsf: meters below sea floor) and the nannofossil zonation of Martini (1971), calibrated to the timescale of Gradstein et al. (2012). LO: Late Oligocene.

Figure 1

Click here to download Figure(s): Figure 1 revised.eps

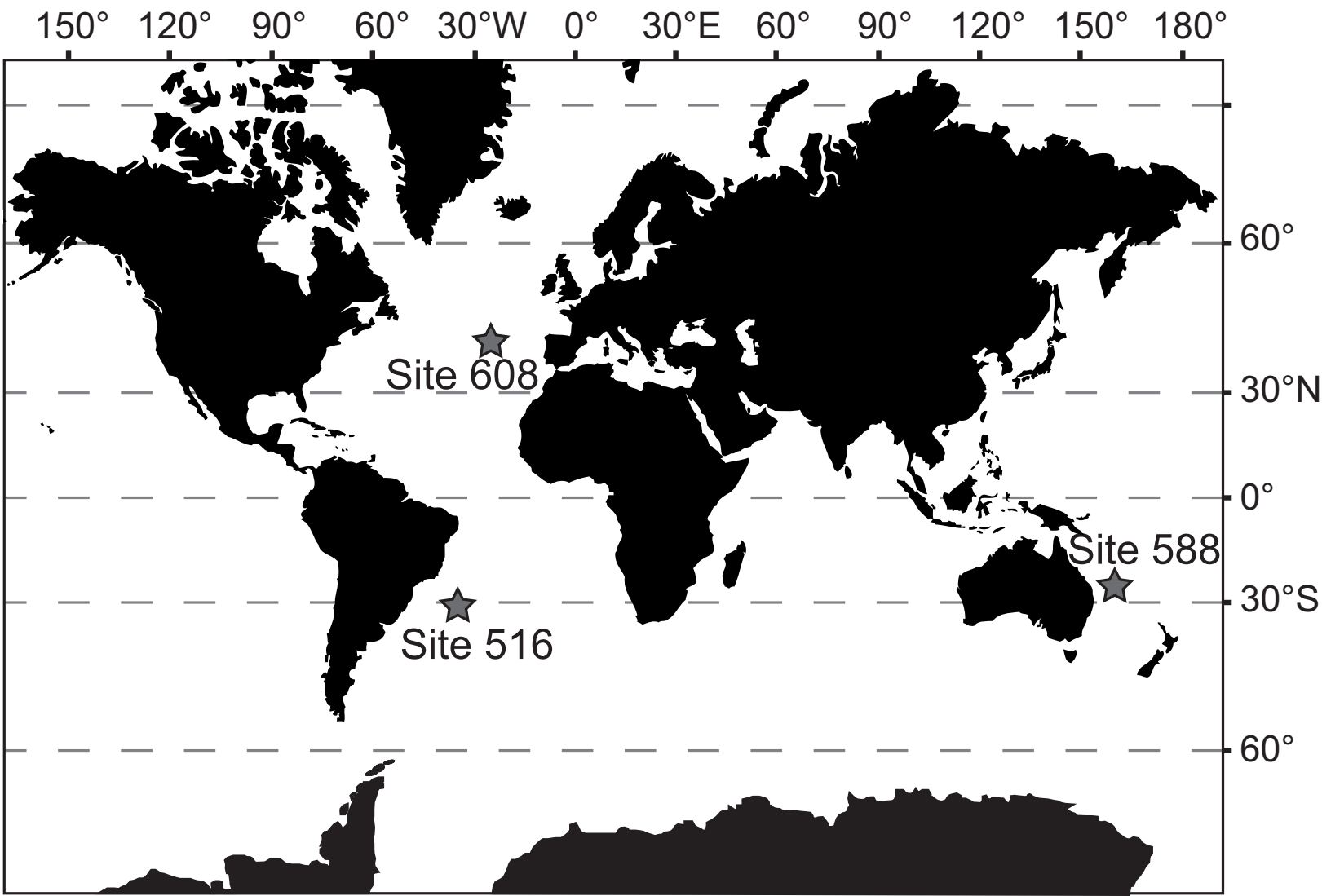

Figure 2

Click here to download Figure(s): Figure 2 revised.eps

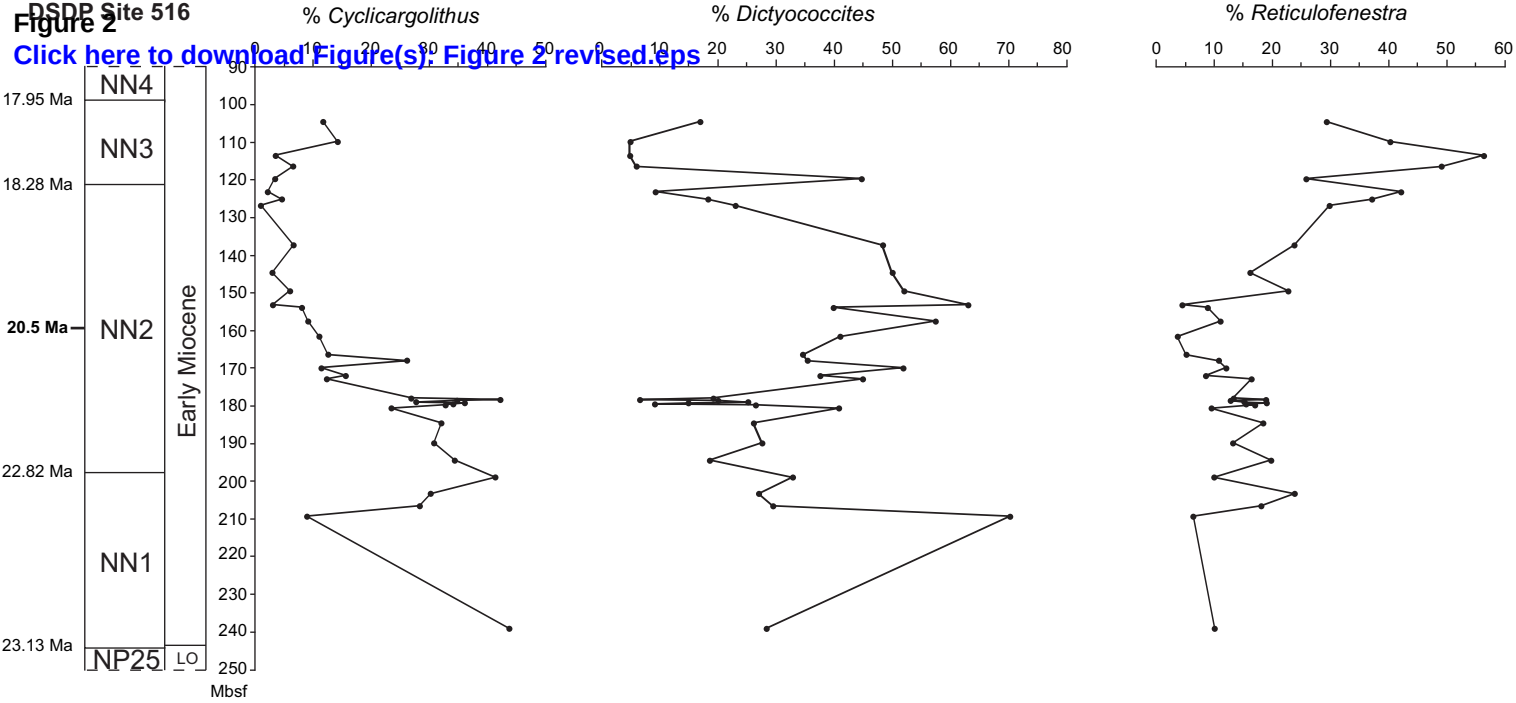

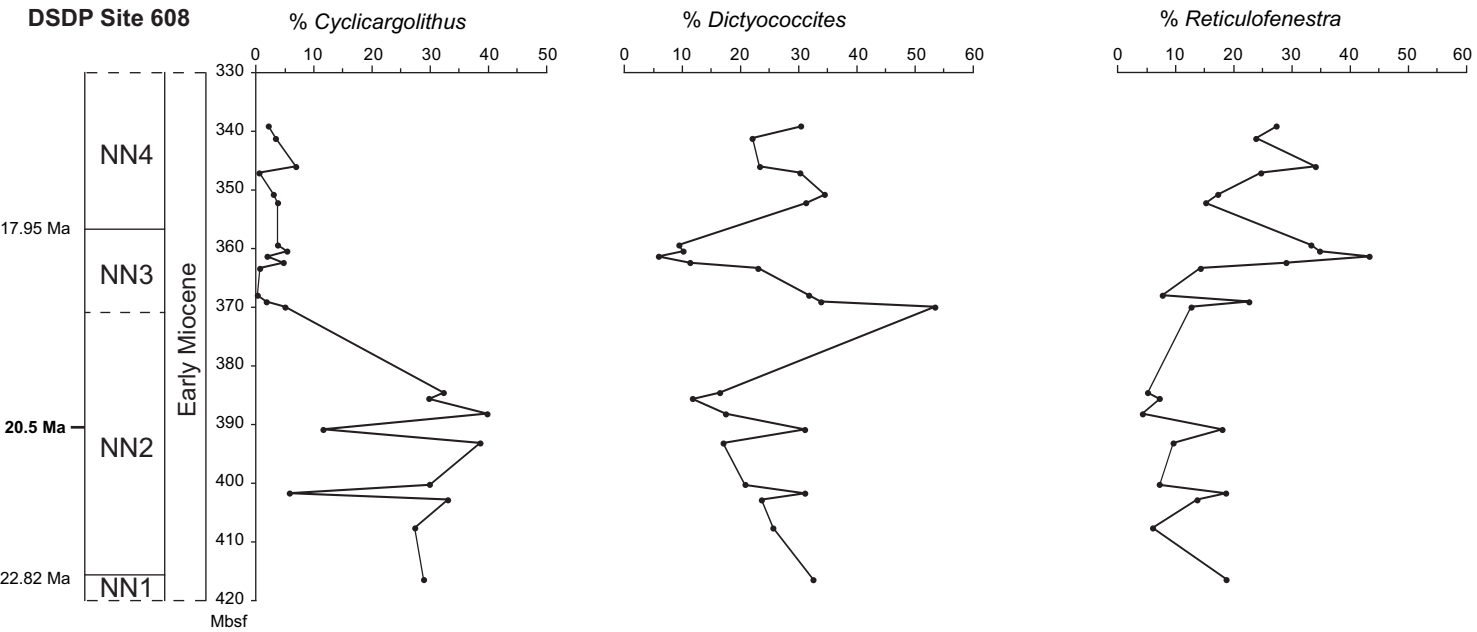

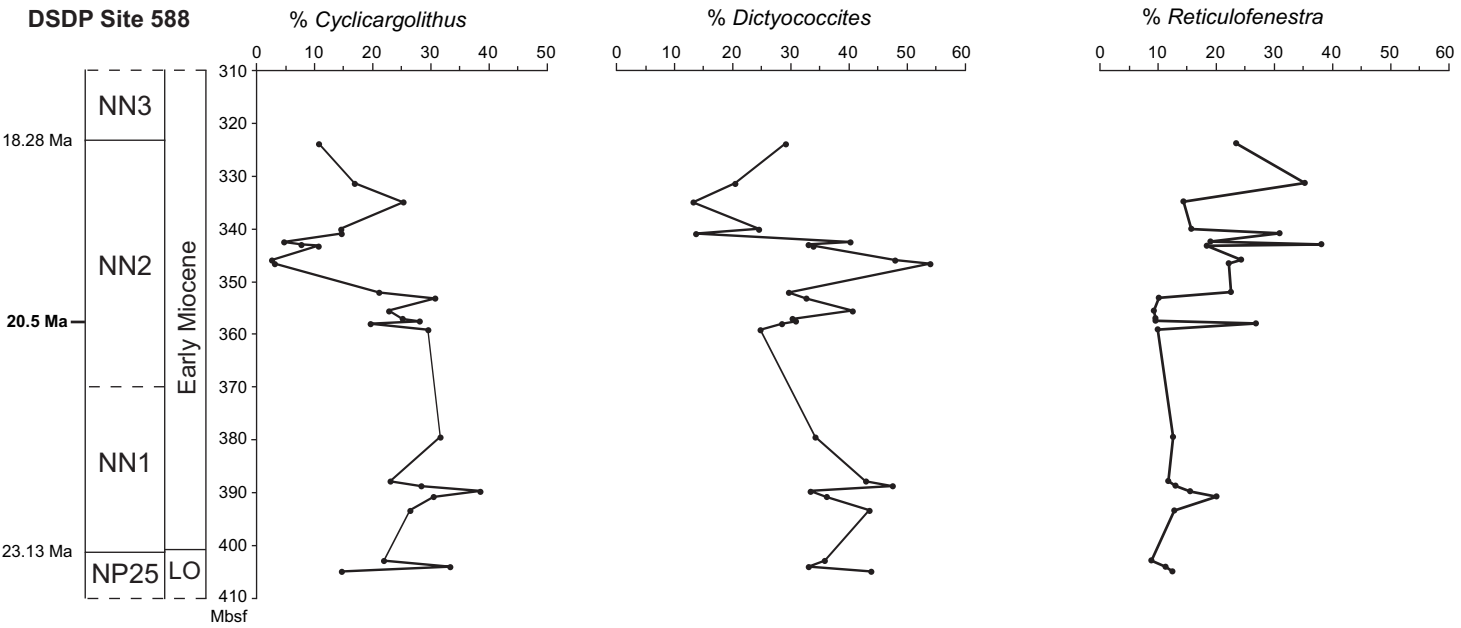

Figure 3

Click here to download Figure(s): Figure 3 revised.eps

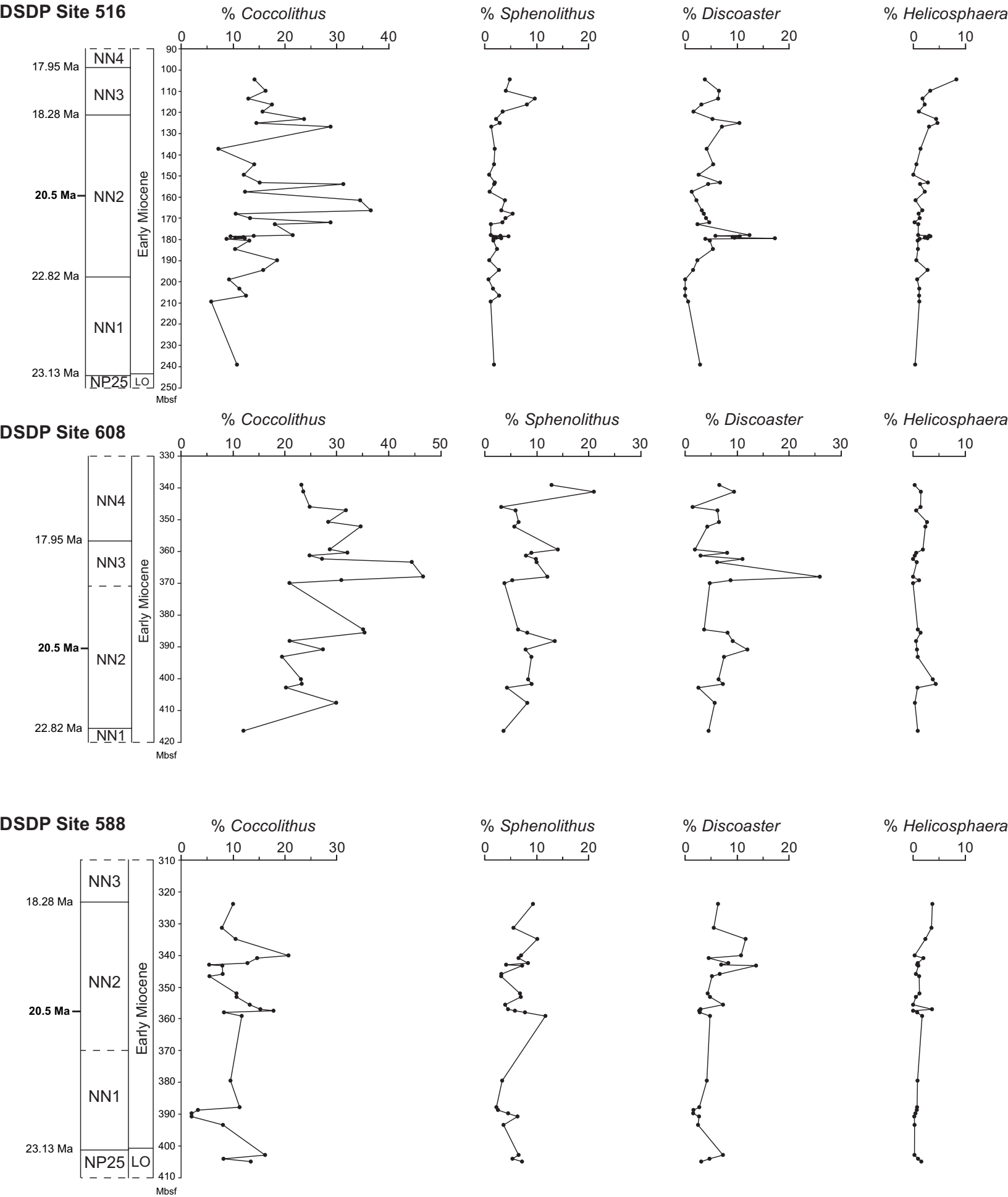

Figure 4

Click here to download Figure(s): Figure 4 revised.eps

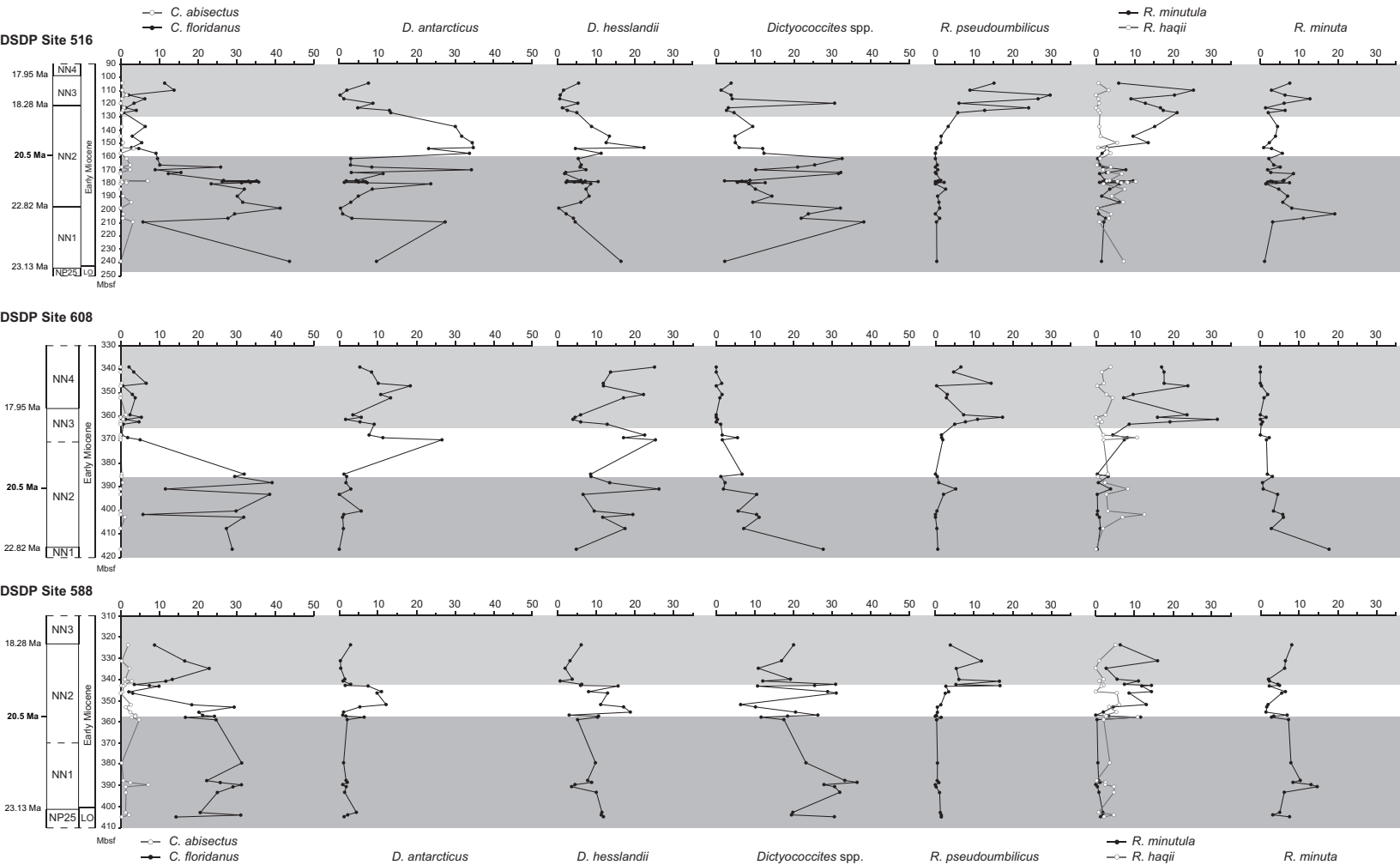

Plate 1

Click here to download Figure(s): Plate 1 revised.eps

a) *Reticulofenestra minutula*

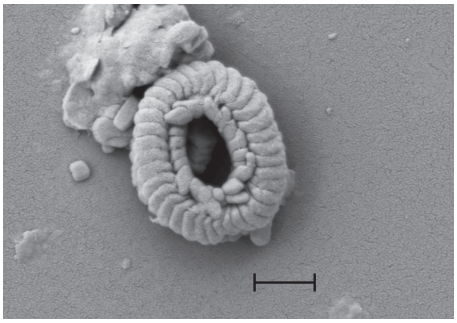

b) *Reticulofenestra minuta*

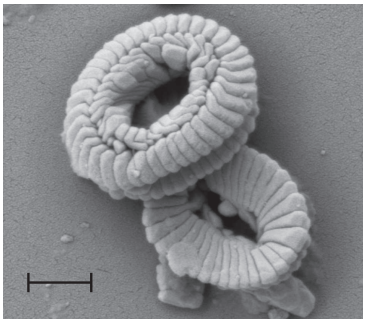

c) *Reticulofenestra minuta*

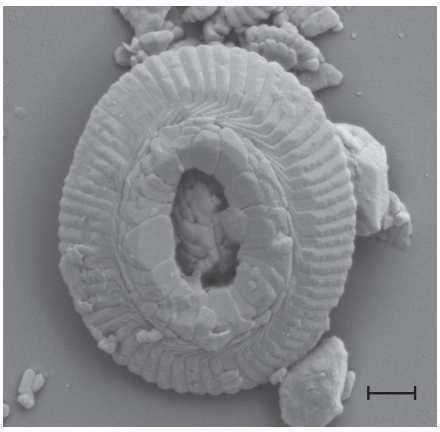

d) *Reticulofenestra pseudoumbilicus*

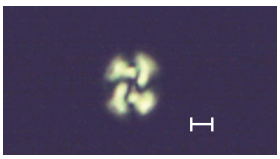

e) *Dictyococcites* sp.

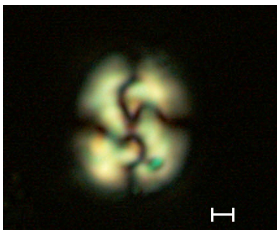

f) *Dictyococcites antarcticus*

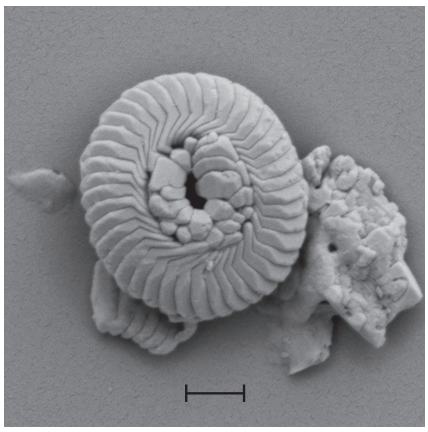

g) *Dictyococcites hesslandii*

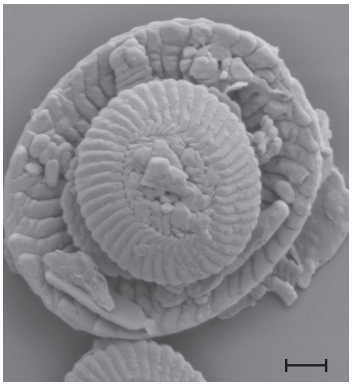

h) *Dictyococcites antarcticus*

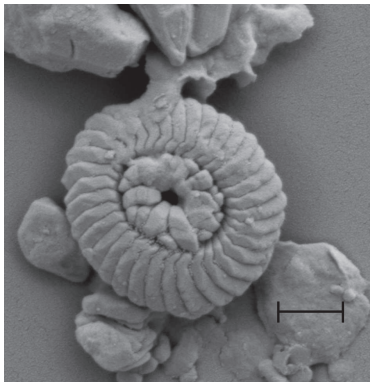

i) *Dictyococcites* sp.

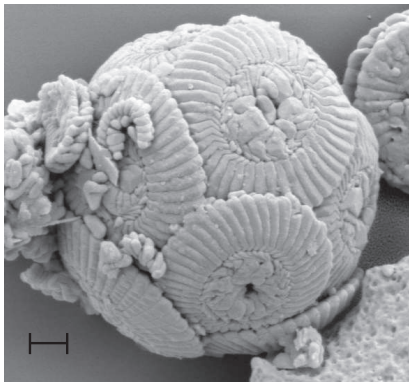

j) *Dictyococcites hesslandii* (coccosphere)

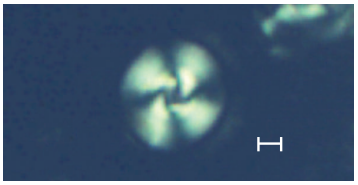

k) *Cyclicargolithus floridanus*

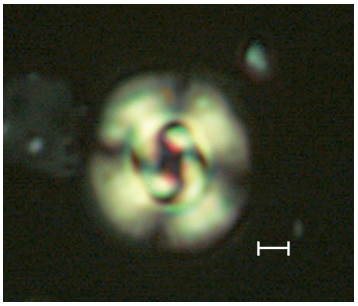

l) *Cyclicargolithus floridanus*

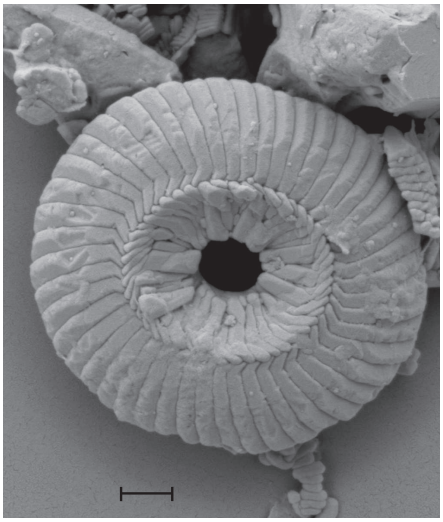

m) *Cyclicargolithus floridanus*

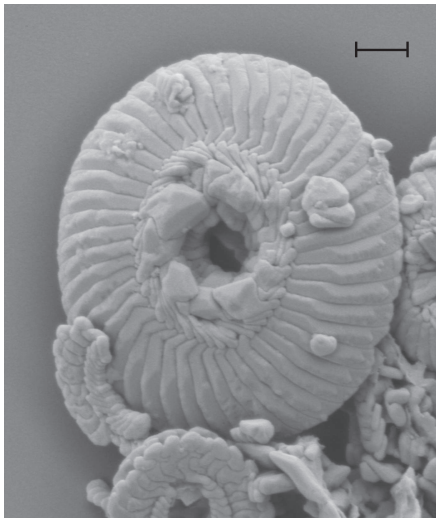

n) *Cyclicargolithus floridanus*

Figure S1

Click here to download Supplementary Data for online publication only: Figure S1 revised.eps

Nannofossil abundance data

Click here to download Supplementary Data for online publication only: Nannofossil abundance data revised.xlsx